Functional malignant cell heterogeneity in pancreatic neuroendocrine tumors revealed by targeting of PDGF-DD

Eliane Cortez[a], Hanna Gladh[b], Sebastian Braun[a], Matteo Bocci[a], Eugenia Cordero[a], Niklas K. Björkström[c], Hideki Miyazaki[a], Iacovos P. Michael[d], Ulf Eriksson[b], Erika Folestad[b], and Kristian Pietras[a,1]

[a]Department of Laboratory Medicine, Lund University, Medicon Village, SE-22381 Lund, Sweden; [b]Department of Medical Biochemistry and Biophysics, Karolinska Institutet, SE-17177 Stockholm, Sweden; [c]Department of Medicine, Karolinska Institutet, SE-14186, Stockholm, Sweden; and [d]Swiss Institute for Experimental Cancer Research, École Polytechnique Fédérale de Lausanne, CH-1015 Lausanne, Switzerland

Edited by Napoleone Ferrara, University of California, San Diego, La Jolla, CA, and approved January 4, 2016 (received for review May 13, 2015)

Intratumoral heterogeneity is an inherent feature of most human cancers and has profound implications for cancer therapy. As a result, there is an emergent need to explore previously unmapped mechanisms regulating distinct subpopulations of tumor cells and to understand their contribution to tumor progression and treatment response. Aberrant platelet-derived growth factor receptor beta (PDGFRβ) signaling in cancer has motivated the development of several antagonists currently in clinical use, including imatinib, sunitinib, and sorafenib. The discovery of a novel ligand for PDGFRβ, platelet-derived growth factor (PDGF)-DD, opened the possibility of a previously unidentified signaling pathway involved in tumor development. However, the precise function of PDGF-DD in tumor growth and invasion remains elusive. Here, making use of a newly generated *Pdgfd* knockout mouse, we reveal a functionally important malignant cell heterogeneity modulated by PDGF-DD signaling in pancreatic neuroendocrine tumors (PanNET). Our analyses demonstrate that tumor growth was delayed in the absence of signaling by PDGF-DD. Surprisingly, ablation of PDGF-DD did not affect the vasculature or stroma of PanNET; instead, we found that PDGF-DD stimulated bulk tumor cell proliferation by induction of paracrine mitogenic signaling between heterogeneous malignant cell clones, some of which expressed PDGFRβ. The presence of a subclonal population of tumor cells characterized by PDGFRβ expression was further validated in a cohort of human PanNET. In conclusion, we demonstrate a previously unrecognized heterogeneity in PanNET characterized by signaling through the PDGF-DD/PDGFRβ axis.

tumor heterogeneity | platelet-derived growth factor-DD | neuroendocrine tumor

Undeniably, cancer progression is the consequence of dynamic, and yet poorly understood, cell–cell interactions driven by frequently deregulated signaling pathways (1). Further complexity arises from the notion that tumors are composed of phenotypically and functionally distinct subsets of both malignant and stromal cells (2, 3). Therefore, accounting for intratumoral heterogeneity poses an additional challenge when designing therapies that can efficiently control or eliminate tumors. An improved understanding of the functional contribution of different signaling pathways to genetic and phenotypic variation within tumors is therefore highly warranted.

Members of the platelet-derived growth factor (PDGF) family and their receptors (PDGFRs) have been extensively investigated and shown to be critical for cellular processes such as proliferation, survival, and motility during tumor growth and invasion (4). The roles of PDGF isoforms and their target cells in tumor development have been charted in different tumor types (5), and as a result, pharmacological blockade of PDGF signaling is now routinely used for the treatment of diverse malignancies, such as gastrointestinal stromal tumors and chronic myelomonocytic leukemia, among others (6, 7). The PDGF family is composed of four polypeptide chains that assemble into five dimeric isoforms (PDGF-AA, PDGF-BB, PDGF-AB, PDGF-CC, and PDGF-DD) that bind and activate two receptor tyrosine kinases (PDGFRα and PDGFRβ) expressed mainly by cells of mesenchymal origin (8). PDGF-DD is the most recently identified member of the family (9, 10), and unlike the other ligands, the role of PDGF-DD in normal development and pathology is largely a conundrum.

Herein, we report the use of a *Pdgfd* knockout mouse to explore the specific role of PDGF-DD in malignant growth. By monitoring tumorigenesis in the RIP1-TAg2 mouse model of pancreatic neuroendocrine tumors (PanNET), we found that disruption of PDGF-DD signaling significantly delayed tumor growth. In the absence of PDGF-DD, functional compensation by PDGF-BB was apparent in the stromal compartment. Unexpectedly, however, we identified a subpopulation of malignant cells expressing PDGFRβ with accompanying responsiveness to PDGF-DD. By modulating PDGFRβ$^+$ malignant cells, PDGF-DD contributes to the maintenance of functional malignant cell heterogeneity in experimental PanNET.

Results

***Pdgfd* Is Predominantly Expressed in the Endothelial Cell Compartment of Tumors from RIP1-TAg2 Mice.** To study the effect of *Pdgfd* depletion in tumor development, we made use of the RIP1-TAg2 transgenic mouse model of multistage PanNET (11). Briefly, pancreatic β-cells

Significance

Emerging evidence suggest that the cellular composition of tumors is highly heterogeneous. Subclonal species of malignant cells may account for variability in therapeutic responses and for relapse following treatments. However, little is known about the molecular drivers of specific subsets of cancer cells. Herein, we identify expression of platelet-derived growth factor receptor beta (PDGFRβ) as a previously unrecognized feature of a minor malignant cell population in pancreatic neuroendocrine tumors. By the use of mice genetically deficient for *Pdgfd*, we reveal a crucial and nonredundant function for signaling by platelet-derived growth factor (PDGF)-DD in promoting functional tumor heterogeneity by providing growth-stimulatory cues. Taken together, the use of drugs targeting PDGFRβ signaling, such as the approved targeted therapy sunitinib, may affect the functional intratumoral cross talk in pancreatic neuroendocrine tumors.

Author contributions: E. Cortez and K.P. designed research; E. Cortez, H.G., S.B., M.B., E. Cordero, E.F., and K.P. performed research; N.K.B., I.P.M., and U.E. contributed new reagents/analytic tools; E. Cortez, H.G., H.M., E.F., and K.P. analyzed data; and E. Cortez and K.P. wrote the paper.

The authors declare no conflict of interest.

This article is a PNAS Direct Submission.

Freely available online through the PNAS open access option.

[1]To whom correspondence should be addressed. Email: kristian.pietras@med.lu.se.

This article contains supporting information online at www.pnas.org/lookup/suppl/doi:10.1073/pnas.1509384113/-/DCSupplemental.

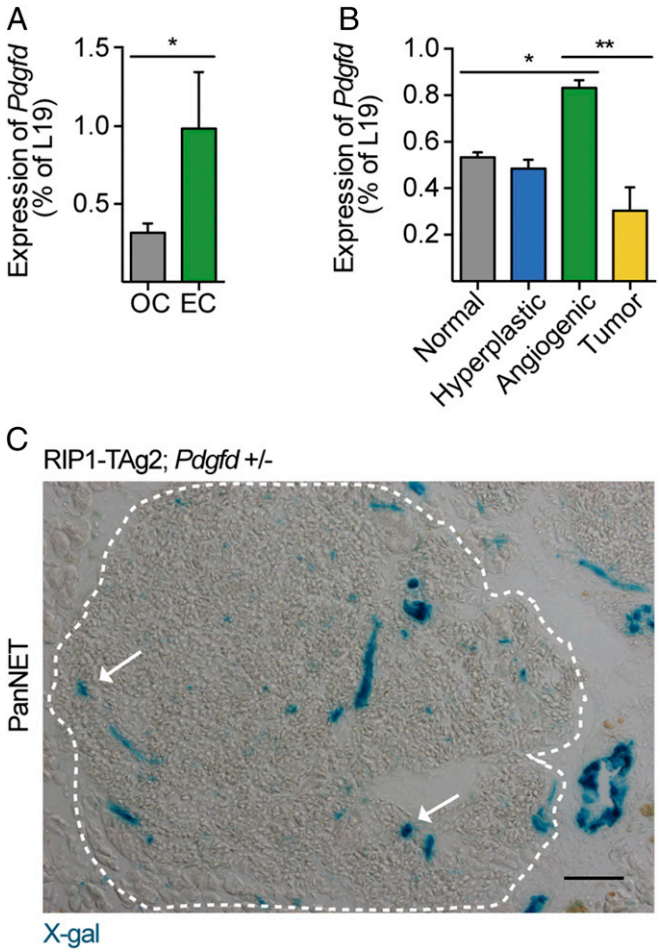

Fig. 1. *Pdgfd* is expressed primarily by endothelial cells in tumors from RIP1-TAg2 mice. (*A*) Quantitative RT-PCR analysis of the expression of *Pdgfd* in endothelial cell (EC) fraction and other cell (OC) fraction isolated from tumors of RIP1-TAg2 mice. Error bars show the mean ± SD. (*B*) qRT-PCR analysis of the expression of *Pdgfd* in pancreatic islets from progressive tumor stages in RIP1-TAg2 mice (material pooled from >20 mice per tumor stage). (*C*) X-gal staining of islet tumor section from RIP1-TAg2;*Pdgfd*$^{+/-}$ mouse. A dashed line delineates the angiogenic islet lesion area. *$P < 0.05$, **$P < 0.01$. (Scale bar, 50 μm.)

in the islets of Langerhans of RIP1-TAg2 mice are engineered to express the oncogenic SV40 T antigens, under the control of the rat insulin promoter, leading to the formation of hyperproliferative islets that progress by activating angiogenesis and ultimately resulting in locally invasive and metastatic tumors. Previous expression profiling of PDGF ligands and receptors in tumors from RIP1-TAg2 mice found *Pdgfd* to be expressed exclusively by endothelial cells (ECs) (12). Consistent with these results, we observed a significant enrichment of *Pdgfd* mRNA in isolated ECs of tumors from RIP1-TAg2 mice, compared with non-ECs (Fig. 1*A*). In addition, when we analyzed the expression pattern of *Pdgfd* during tumorigenesis in RIP1-TAg2 mice, we found *Pdgfd* to be significantly up-regulated in angiogenic islets, compared with other stages of normal or malignant islets (Fig. 1*B*), an expression pattern previously found to be characteristic for genes expressed by ECs (13). Next, we generated a mouse line in which the *Pdgfd* exon 1 was substituted for a LacZ reporter cassette, allowing for monitoring of gene expression by X-gal staining. Using tumor tissue sections from compound RIP1-TAg2;*Pdgfd*$^{+/-}$ mice, we detected robust LacZ activity in large vessels, as well as weaker signal in microvascular structures within the tumor parenchyma (Fig. 1*C*, arrows). Taken together, these observations suggest that in the RIP1-TAg2 tumor model, ECs are the predominant source for PDGF-DD.

***Pdgfd* Deficiency Delays Tumor Growth, Leading to Prolonged Survival.** Mice homozygous for the inactivated *Pdgfd* allele (*Pdgfd*$^{-/-}$ mice) are viable and fertile and do not display any obvious discrepancies in the histology or insulin secretion of the islets of Langerhans, compared with *Pdgfd*$^{+/+}$ littermates (Fig. 2*A*). We next evaluated the tumorigenic progression of RIP1-TAg2;*Pdgfd*$^{+/-}$ and RIP1-TAg2;*Pdgfd*$^{-/-}$ mice to that of RIP1-TAg2;*Pdgfd*$^{+/+}$ littermates. First, we examined the effect of impaired *Pdgfd* expression on the activation of the angiogenic switch by quantifying the number of angiogenic islets and tumors present in the pancreas of 12-wk-old RIP1-TAg2 mice. Our analysis revealed a similar number of both angiogenic islets and tumors regardless of genotype (Fig. 2 *B* and *C*), suggesting that PDGF-DD does not affect the progression of tumors from premalignant angiogenic lesions into overt tumors. In sharp contrast, both RIP1-TAg2;*Pdgfd*$^{+/-}$ and RIP1-TAg2;*Pdgfd*$^{-/-}$ mice presented with a significantly reduced total tumor burden (29.5 ± 18 mm^3 and 25.7 ± 21.1 mm^3, respectively) compared with RIP1-TAg2;*Pdgfd*$^{+/+}$ mice (71.9 ± 68 mm^3) (Fig. 2*D*). Consistent with the decrease in tumor burden, RIP1-TAg2;*Pdgfd*$^{+/-}$ and RIP1-TAg2;*Pdgfd*$^{-/-}$ mice also showed significantly prolonged median survival (15.9 wk and 15.4 wk, respectively) compared with RIP1-TAg2;*Pdgfd*$^{+/+}$ littermates (13.7 wk) (Fig. 2*E*).

***Pdgfd* Ablation Reduces Tumor Cell Proliferation but Does Not Affect the Invasive or Metastatic Properties of Tumors from RIP1-TAg2 Mice.** To investigate whether the diminished tumor size in tumors from RIP1-Tag2;*Pdgfd*$^{-/-}$ mice was due to an increase in apoptosis or a decrease in proliferation, we stained tumor tissue sections for cleaved caspase-3, an apoptotic cell marker (Fig. 3 *A* and *B*), and assessed the proliferative rate by injecting mice with BrdU (Fig. 3 *C* and *D*). No change was observed when we quantified apoptotic cells in tumors from RIP1-TAg2;*Pdgfd*$^{-/-}$ mice compared with RIP1-TAg2;*Pdgfd*$^{+/+}$ controls (Fig. 3*B*). In contrast, we detected a considerable decrease of 69% in proliferating BrdU$^+$ cells in tumors from RIP1-TAg2;*Pdgfd*$^{-/-}$ compared with RIP1-TAg2;*Pdgfd*$^{+/+}$ littermates (Fig. 3*D*). An increasing number of studies propose that PDGF-DD regulates the process of epithelial-to-mesenchymal transition (EMT), an event preceding metastatic spread (14). Hematoxylin/eosin (H&E) staining of liver tissue sections (Fig. S1*A*) revealed that the number of hepatic micrometastatic lesions was not different in RIP1-TAg2;*Pdgfd*$^{-/-}$ mice compared with RIP1-TAg2;*Pdgfd*$^{+/+}$ mice (Fig. S1*B*). Furthermore, visualization of local tumor invasion, as determined by the border of the pancreatic endocrine lesion (assessed by immunostaining for insulin) with the surrounding exocrine tissue (assessed by immunostaining for α-amylase) demonstrated that tumors invaded the adjacent exocrine tissue to the same extent, regardless of *Pdgfd* expression (Fig. S1*C*).

Angiogenesis, Pericyte Recruitment, and Immune Cell Infiltration Are Not Affected by PDGF-DD Inhibition. Given the reported effect of PDGF ligands on tumor angiogenesis in general and pericyte recruitment in particular (15), we characterized the vascular phenotype of tumors in RIP1-TAg2 mice following *Pdgfd* disruption. The vascular density, as shown by immunostaining for the luminal vessel marker podocalyxin (Fig. S2*A*), was unchanged upon blunted *Pdgfd* expression (Fig. S2*B*). Similarly, tumor vessel perfusion, measured in mice that were systemically administered with fluorescein-coupled tomato lectin before sacrifice, was not significantly affected by the absence of PDGF-DD (Fig. S2 *C* and *D*). The role of PDGF-BB, the prototypical ligand for PDGFRβ, in recruitment of pericytes to the tumor vasculature in RIP1-TAg2 mice has been previously described (16). Therefore, we asked whether PDGF-DD would have a similar effect on pericyte recruitment to tumor blood vessels. By immunostaining, we analyzed tumor sections from RIP1-TAg2 mice

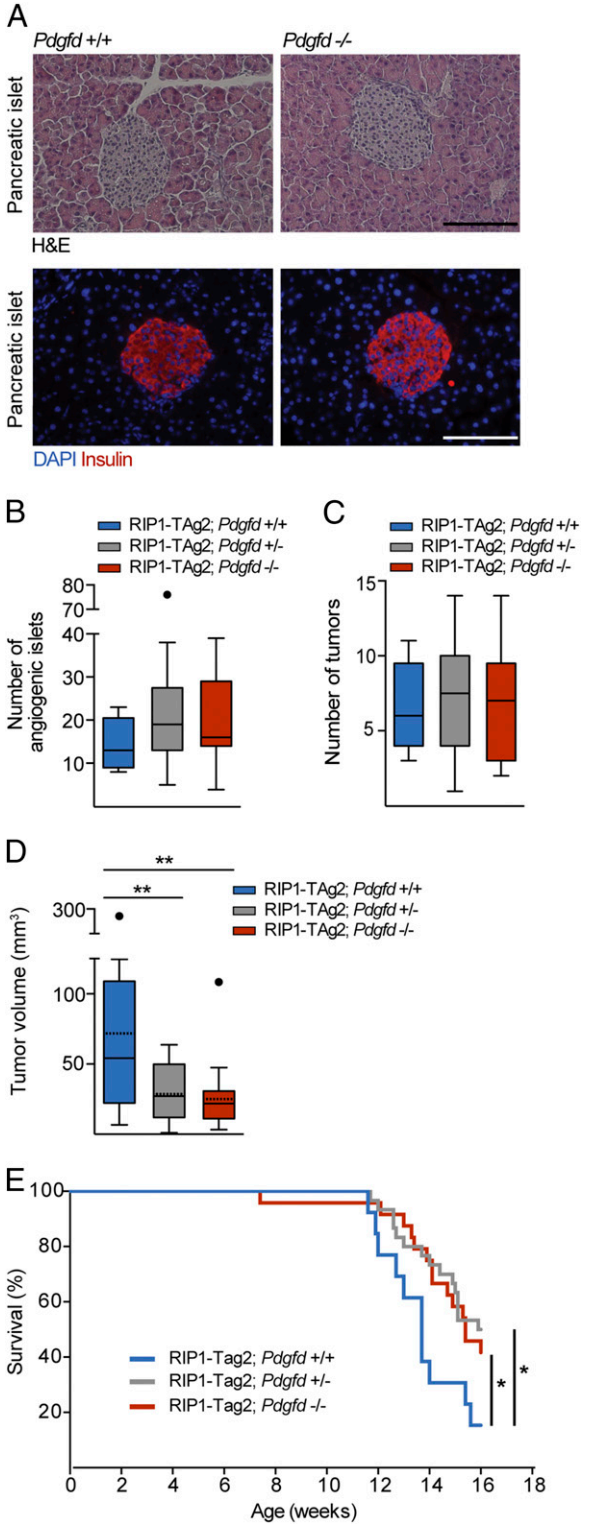

Fig. 2. *Pdgfd* deficiency delays tumor growth, leading to prolonged survival. (*A*) Representative images of islets of Langerhans from *Pdgfd*$^{+/+}$ and *Pdgfd*$^{-/-}$ mice used for assessment of histology, demonstrated by H&E staining, and functionality, shown by immunostaining for insulin (red) to visualize secretion and distribution. Nuclei were stained with DAPI in *Lower*. (Scale bar, 100 μm.) (*B*) Quantification of the number of angiogenic islets, (*C*) the number of tumors, and (*D*) total tumor burden in 12-wk-old RIP1-TAg2;*Pdgfd*$^{+/+}$ (n = 17), RIP1-TAg2;*Pdgfd*$^{+/-}$ (n = 26), and RIP1-TAg2;*Pdgfd*$^{-/-}$ (n = 25) mice. Boxes represent the interquartile range, and the bars represent the full range. Solid lines represent median values and dashed lines represent mean values. Full circles denote statistical outliers. (*E*) Survival of RIP1-TAg2;*Pdgfd*$^{+/+}$ (blue line; median survival = 13.7 wk, n = 13), RIP1-TAg2;*Pdgfd*$^{+/-}$ (gray line; median survival = 15.9 wk, n = 30, $P < 0.05$), and RIP1-TAg2;*Pdgfd*$^{-/-}$ (red line; median survival = 15.4 wk, n = 24, $P < 0.05$) mice. Error bars show the mean ± SD. *$P < 0.05$, **$P < 0.01$.

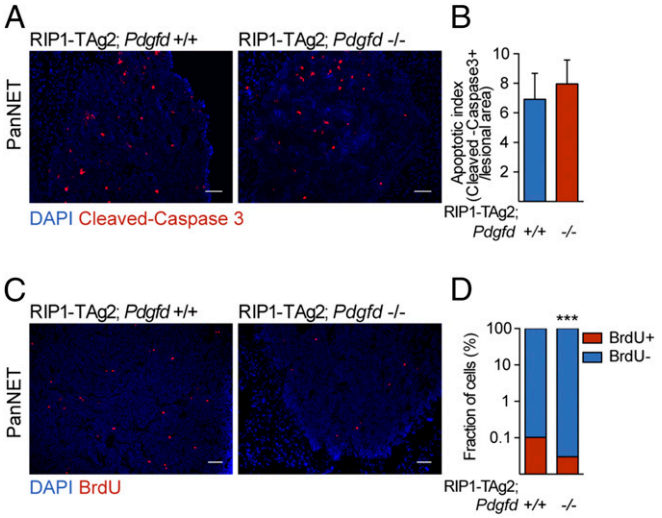

Fig. 3. *Pdgfd* deficiency does not affect cell apoptosis, but reduces tumor cell proliferation in tumors from RIP1-TAg2 mice. (*A* and *B*) Apoptotic index assessed by cleaved-caspase 3 immunostaining and (*C* and *D*) proliferation assessed by BrdU immunostaining of tumor sections from RIP1-TAg2;*Pdgfd*$^{+/+}$ (n = 4) and RIP1-TAg2;*Pdgfd*$^{-/-}$ (n = 6). Seven to twelve islet lesions were assessed for each mouse. The number of apoptotic and proliferating cells was determined by quantification of the positively stained cells in relation to the total tumor lesion area (mm^2) or total number of cells/lesion, respectively. Error bars show the mean ± SD. ***$P < 0.001$. (Scale bars, 50 μm.)

for the expression of well-characterized markers denoting different subsets of pericytes, i.e., PDGFRβ, NG2, and desmin (2, 17, 18) (Fig. 4*A*). Unexpectedly, pericyte coverage was unchanged in the tumor vasculature of RIP1-TAg2;*Pdgfd*$^{+/-}$ and RIP1-TAg2;*Pdgfd*$^{-/-}$ mice compared with RIP1-TAg2;*Pdgfd*$^{+/+}$ mice (Fig. 4*B*). However, we observed in rare malignant lesions that PDGFRβ^{+} peri-vascular cells in tumors from RIP1-TAg2;*Pdgfd*$^{-/-}$ mice appeared more detached from the abluminal endothelial surface in blood vessels, compared with tumors from RIP1-TAg2;*Pdgfd*$^{+/+}$ mice (Fig. 4*A*, arrows). Given that the increased detachment did not correlate with changes in vessel density or functionality (Fig. S2 *A–D*), we concluded that pericyte detachment was most likely not sufficient to account for the differences in tumor size observed upon impairment of *Pdgfd* expression.

Additionally, in a mouse model of wound healing, *Pdgfd* overexpression was accompanied by an increased recruitment of macrophages (19), a cell type associated with the angiogenic phenotype in tumors from RIP1-TAg2 mice (20). However, the immune profile of RIP1-TAg2 mice characterized by immunostaining of tumor tissue sections for a general leukocyte marker (CD45) and a macrophage marker (F4/80) did not give any evidence for gross differences in the infiltration of inflammatory cells upon *Pdgfd* deletion (Fig. S3 *A–D*).

Identification of a Subset of Malignant Pancreatic β-Cells Expressing PDGFRβ in RIP1-TAg2 Mice. Because we did not detect major alterations in the tumor stroma of PanNET lesions from RIP1-TAg2 mice following *Pdgfd* depletion, we profiled the expression of PDGF family members by quantitative RT-PCR (qRT-PCR). Notably, we found that the level of *Pdgfb* transcript was significantly increased in tumors from RIP1-TAg2;*Pdgfd*$^{-/-}$ mice compared with RIP1-TAg2;*Pdgfd*$^{+/+}$ mice (Fig. 5), suggesting a compensatory effect due to the lack of PDGF-DD. Nevertheless, the up-regulation

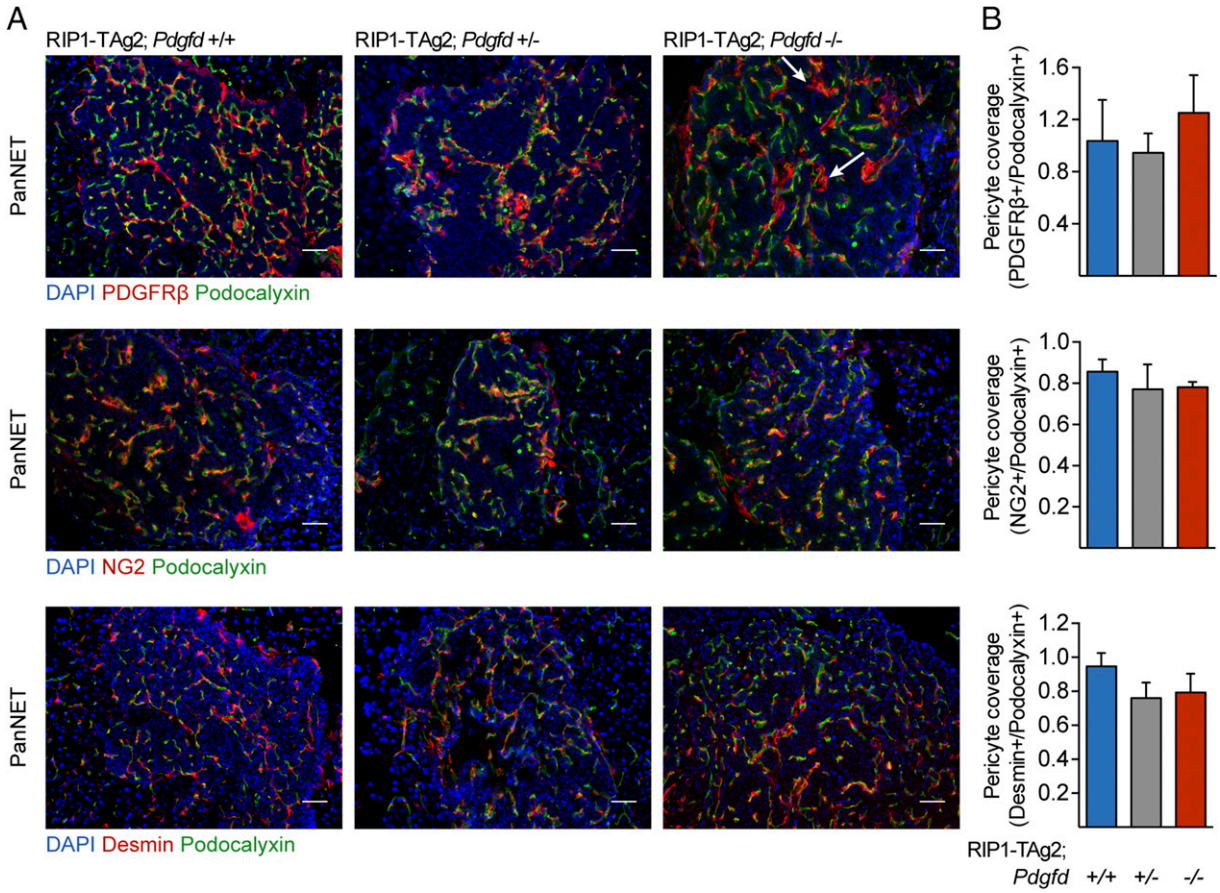

Fig. 4. Pericyte recruitment is not affected by PDGF-D ablation in tumors of RIP1-TAg2 mice. (*A* and *B*) Pericyte coverage quantification in tumor sections from RIP1-TAg2;*Pdgfd*$^{+/+}$, RIP1-TAg2;*Pdgfd*$^{+/-}$, and RIP1-TAg2;*Pdgfd*$^{-/-}$ mice based on immunostaining for pericyte markers NG2, PDGFRβ, and desmin (red) in relation to the endothelial cell marker podocalyxin (green). Cell nuclei were visualized using DAPI (blue) ($n = 3$ mice per group). Error bars show the mean ± SD. (Scale bars, 50 μm.)

of *Pdgfb* was still unable to rescue the observed reduction in overall tumor size, indicative of a specific role for PDGF-DD signaling during PanNET development. Therefore, we explored alternative mechanisms that could account for the significant reduction in tumor size. We speculated that there might exist cell types outside of the perivascular compartment responsive to PDGF-DD by expression of PDGFRβ. Consequently, we performed immunostaining of tumor and liver tissue sections from RIP1-TAg2 mice for PDGFRβ and insulin or T-Antigen to label malignant cells. We identified rare cells coexpressing PDGFRβ and insulin in primary tumors (Fig. 6*A*, *Right*), consistent with previous reports of activated PDGFRβ in whole tumor lysates of human PanNET lesions (21). Malignant cells expressing PDGFRβ were more prevalent in micrometastatic lesions in the liver (Fig. 6 *B* and *C*). To further confirm the observation of PDGFRβ^{+} malignant β-cells, we prepared a single-cell suspension from tumors of RIP1-TAg2 mice and ex vivo labeled the cells with fluorescently coupled Exendin 4, a peptide ligand for the glucagon-like peptide 1 receptor (GLP1R), which is selectively expressed by β-cells in the endocrine pancreas (22). By analyzing the cells using fluorescence activated cell sorting (FACS), we detected a subpopulation of cells (~0.3–0.8% depending on the tumor) coexpressing GLP1R and PDGFRβ (Fig. 6*D*). We also made use of double transgenic RIP1-Tag2;PDGFRβ-EGFP mice (23), which faithfully produce the fluorescent marker in cells expressing PDGFRβ (Fig. 6*E*). Analysis of single-cell suspensions of PanNET from compound RIP1-TAg2; PDGFRβ-EGFP mice by FACS corroborated the occurrence of a minor population of malignant cells expressing PDGFRβ (Fig. 6*F*).

In parallel with the in vivo characterization, we validated our findings using various pancreatic β-tumor cell lines. First, we performed qRT-PCR analysis and detected *Pdgfrβ* transcripts in malignant βTC3 cells (24), premalignant βHCII cells, and additional cell lines established from tumors of RIP1-TAg2 mice (βTC PO, βTC-99-3o, and βTC-1710-1) (Fig. 7*A*). Furthermore, to confirm the expression of PDGFRβ, we immunostained βTC3 cells and detected strongly positive staining on rare cells, indicating high expression of PDGFRβ by a subpopulation of cells, rather than a widespread low expression (Fig. 7*B*). Finally, we established the coexistence of PDGFRβ^{+} and PDGFRβ^{-} cells in βTC3 cultures by FACS (Fig. 7*C*). In parallel analyses, no cells expressing PDGFRα were detected

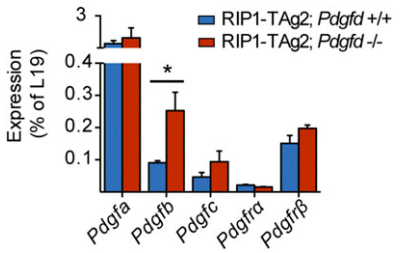

Fig. 5. *Pdgfb* is up-regulated in tumors of RIP1-TAg2;*Pdgfd*$^{-/-}$ mice. Analysis of *Pdgfa, Pdgfb, Pdgfc, Pdgfrα*, and *Pdgfrβ* mRNA expression by qRT-PCR in tumors of RIP1-TAg2;*Pdgfd*$^{+/+}$ and RIP1-TAg2;*Pdgfd*$^{-/-}$ mice ($n = 3$ mice per group). Error bars show the mean ± SD. *$P < 0.05$.

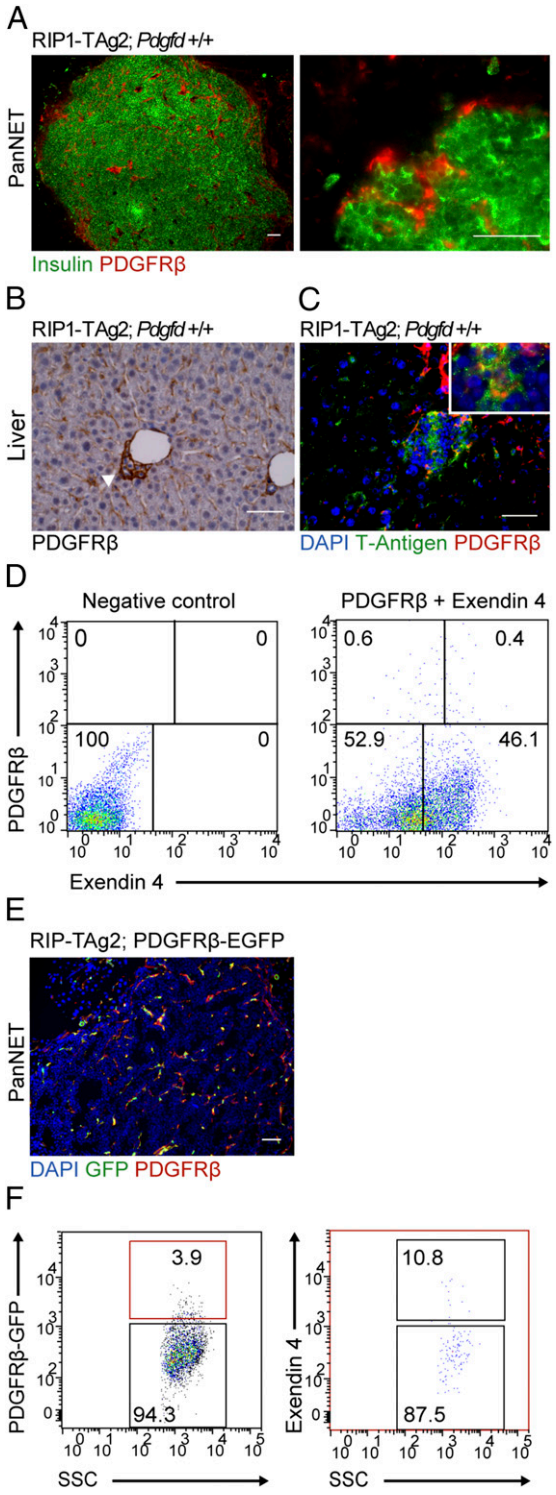

Fig. 6. Identification of a subset of malignant cells expressing PDGFRβ in RIP1-TAg2 tumors. (*A*) Immunostaining of tumor from RIP1-TAg2 mouse for malignant tumor cells (insulin; green) and PDGFRβ (red). (*B* and *C*) Expression of PDGFRβ by malignant cells in liver metastatic lesions of RIP1-TAg2 mice by (*B*) immunohistochemistry (arrow) and (*C*) immunofluorescence by costaining with T-Antigen (T-Ag). (*D*) Quantification of PDGFRβ$^+$/GLP1R$^+$ cell populations in RIP1-TAg2 pancreatic tumors. Tumors were dispersed into single cells, incubated with fluorescently labeled antibody for PDGFRβ (APC) and peptide-ligand, Exendin 4 (FAM), and analyzed by FACS. (*E*) Immunostaining of tumors from RIP1-TAg2;PDGFRβ-EGFP compound mice with PDGFRβ antibody (red) to determine colocalization with EGFP (green) expressed by PDGFRβ cells. (*F*) Flow cytometry gating strategy to analyze double positive Exendin 4$^+$/PDGFRβ-EGFP$^+$ subpopulation of tumor cells in single-cell suspension prepared from tumors of RIP1-TAg2;PDGFRβ-EGF mice. (Scale bars, 50 μm.)

by flow cytometry or immunostaining, illustrating the specific expression of PDGFRβ (Fig. S4 *A*–*C*). Similarly, at the mRNA level, βTC3 express very low levels of *Pdgfrα*, compared with *Pdgfrβ* (Fig. S4*D*). Taken together, both our in vivo and in vitro analyses indicate that although most malignant β-cells are PDGFRβ$^-$, a subset of pancreatic β-tumor cells readily expresses PDGFRβ.

βTC3 Cells Respond to PDGF-DD, but Not PDGF-BB, Stimulation with Increased Proliferation. Next, we tested whether PDGFRβ$^+$ βTC3 cells responded to PDGF-DD. We treated βTC3 cells with recombinant PDGF-DD protein and assessed cell proliferation by phospho-Histone H3 immunostaining (Fig. 7 *D* and *E*). We found that PDGF-DD induced a significant increase in the total number of cells by 37%, and the number of cells positively stained for phospho-Histone H3 was 2.4-fold higher compared with control cultures (Fig. 7*E*). Surprisingly, the prototypical ligand for PDGFRβ, i.e., PDGF-BB, did not augment the proliferation of βTC3 cells (Fig. 7*E*). Because costaining for PDGFRβ and phospho-Histone H3 demonstrated that it was predominantly PDGFRβ$^-$ cells in the vicinity of quiescent PDGFRβ$^+$ cells that were engaged in mitosis (Fig. 7*F*), we reasoned that the effect may be indirect through paracrine secretion of mitogenic factors by PDGFRβ$^+$ cells in response to PDGF-DD stimulation. To test this proposition, we assessed the expression of candidate known mitogens for malignant PanNET cells from RIP1-TAg2 mice following stimulation with PDGF-DD. Indeed, the expression of *Igf1* and *Hgf*, but not of *Igf2* or *Egf*, was significantly induced in βTC3 cells stimulated with PDGF-DD (Fig. 7*G*). Subsequently, to define the characteristics of PDGFRβ-expressing malignant β-cells, we tested whether PDGF-DD induced tumor-initiating capacity. We found that βTC3 cells stimulated by PDGF-DD, but not by PDGF-BB, in anchorage-independent conditions formed a significantly higher number of tumor spheroids, compared with untreated βTC3 control cells (Fig. 7*H*). Additionally, to investigate the tumorigenic properties of PDGFRβ$^+$ βTC3 cells, we sorted cells by FACS based on their expression of PDGFRβ and transplanted subcutaneously (sc) into NOD-SCID mice. Injection of as few as 200 PDGFRβ$^-$ or PDGFRβ$^+$ βTC3 cells resulted in tumor establishment and progressive growth in three out of four mice and two out of four mice, respectively. The resulting histology of tumors from PDGFRβ$^+$ cells was indistinguishable from that of tumors established from PDGFRβ$^-$ βTC3 cells (Fig. 7*I*, *Upper*). In addition, the expression of PDGFRβ in the parenchyma of tumors was similar regardless of cell of origin, indicating interconversion between the different subsets of βTC3 cells (Fig. 7*I*, *Lower*). Furthermore, FACS analysis revealed that tumors established from PDGFRβ$^-$ cells reestablished the original relationship between PDGFRβ$^-$ and PDGFRβ$^+$ malignant cells (Fig. 8*A*). To corroborate this finding, we investigated the prevalence of PDGFRβ$^-$ and PDGFRβ$^+$ malignant cells in βTC3 cultures. We isolated PDGFRβ$^-$ PanNET cells from βTC3 cultures, and after immediately verifying the purity of the cell suspension, cells were propagated for 7 d. Flow cytometric analysis of the resulting culture for PDGFRβ demonstrated the occurrence of a mixed population of cells with the original frequencies, indicative of rapid conversion of PDGFRβ$^-$ malignant cells into PDGFRβ$^+$ (Fig. 8*B*).

Altogether, our comprehensive analyses of the first *Pdgfd*-deficient mouse model of cancer to our knowledge demonstrate that functional malignant cell heterogeneity in experimental PanNET is reinforced by PDGF-DD by stimulation of a subset of tumor cells expressing PDGFRβ that engages in paracrine cross talk with neighboring malignant cells. However, although PDGF-DD stimulates some features of cancer stem cells in PDGFRβ$^+$ PanNET cells, the tumor-initiating capacity is not exclusive to this subset of malignant cells.

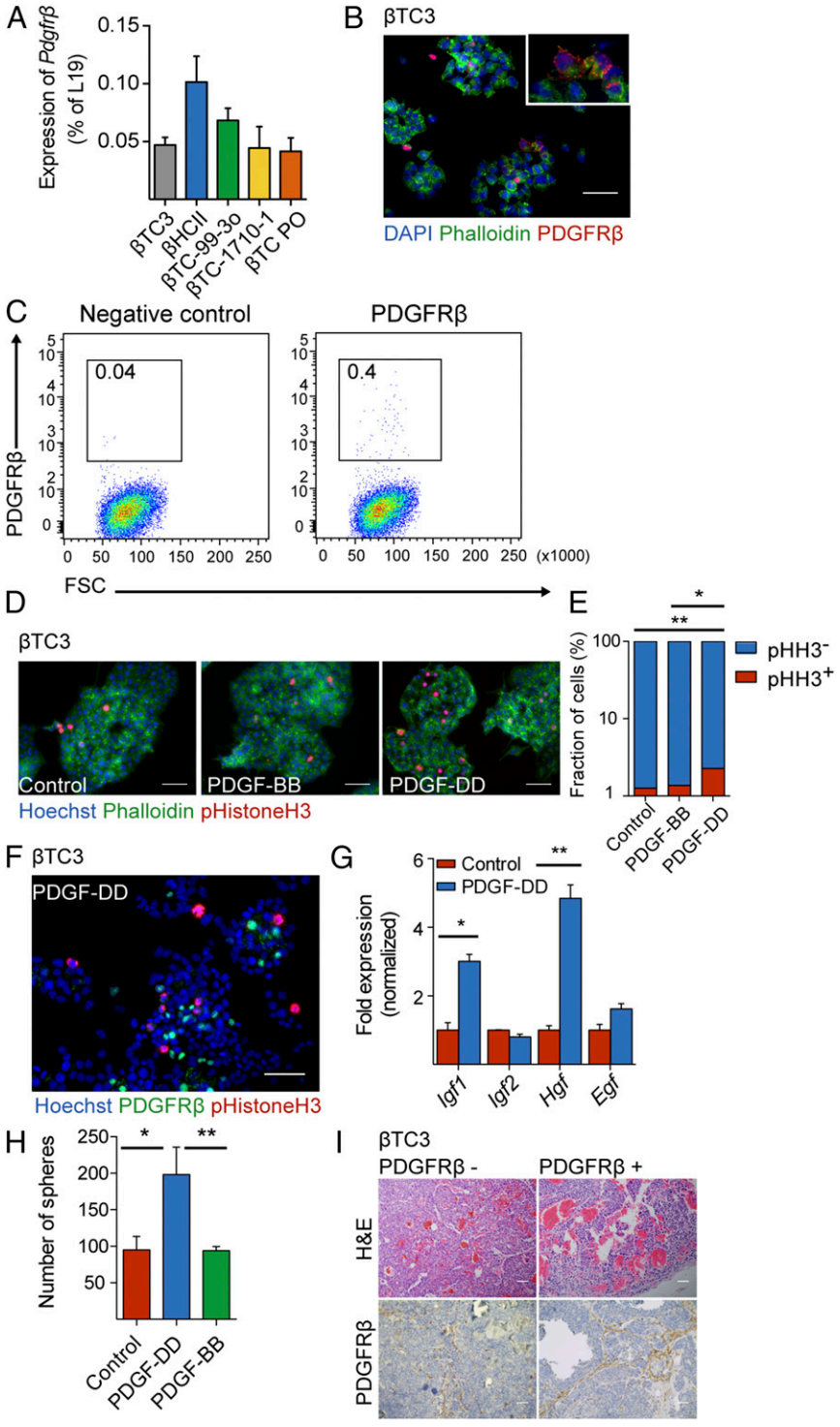

Fig. 7. βTC3 cells expressing PDGFRβ are responsive to PDGF-DD stimulation in vitro. (*A*) Quantitative RT-PCR analysis of the expression of *Pdgfrß* in different βTC lines derived from tumors of RIP1-TAg2 mice. (*B*) Immunostaining of βTC3 with a PDGFRβ antibody (red) and phalloidin (green). Cell nuclei were stained with DAPI. (*C*) Flow cytometry analysis of expression of PDGFRβ in βTC3 cell line using an APC fluorescently labeled antibody. (*D*) Quantification of proliferating βTC3 upon stimulation with PDGF-DD and PDGF-BB assessed by immunostaining with phospho-Histone H3 antibody (red) and phalloidin (green). Cell nuclei were stained with Hoechst. (*E*) The number of proliferating cells was determined by counting the number of phosho-Histone H3$^+$ cells in relation to the total number of cells (Hoechst$^+$). (*F*) Costaining of βTC3 cells with antibodies against phospho-Histone H3 (red) and PDGFRβ (green). Cell nuclei were stained with Hoechst. (*G*) Quantitative RT-PCR analysis of growth factors expressed by βTC3 upon 6 h of stimulation with PDGF-DD. (*H*) Quantification of tumor spheroids formed by βTC3, seeded in anchorage-independent conditions, upon treatment with PDGF-DD and PDGF-BB. (*I*) Analysis of tumors formed from βTC3 cells transplanted into NOD-SCID mice. Hematoxylin/eosin stainings (*Upper*) and immunohistochemistry staining of PDGFRβ (*Lower*) of tumors from PDGFRβ$^-$ βTC3 and PDGFRβ$^+$ βTC3 transplanted cells. Error bars show the mean ± SD. Scale bars, 50 μm. $^*P < 0.05$, $^{**}P < 0.01$.

Human PanNET Harbor a Subset of PDGFRβ$^+$ Malignant Cells. Finally, we analyzed the expression of PDGFRβ in human PanNET and their hepatic metastases by immunostaining. The normal pancreatic islet and liver parenchyma displayed expression of PDGFRβ exclusively in perivascular locations (Fig. 9 *A* and *B*). In contrast, all primary PanNET and hepatic metastases analyzed ($n = 5$ of each) exhibited a subset of malignant cells readily expressing PDGFRβ evenly distributed in the tissue (Fig. 9 *C*–*F*). Although all malignant lesions harbored PDGFRβ$^+$ tumor cells, the relative abundance was variable with some lesions containing more (Fig. 9 *E* and *F*) and others fewer (Fig. 9 *C* and *D*). The PDGFRβ$^+$ tumor cells were distinguishable from pericytes (Fig. 9*G*, arrowheads) by the coexpression of chromogranin A, a widely used marker for malignant cells of neuroendocrine origin (Fig. 9*G*, arrows) (25).

Discussion

An emergent number of preclinical reports suggest that PDGF-DD is a key player in tumor formation by regulating various cellular processes, such as macrophage and stromal cell recruitment (19, 26), EMT (14, 27, 28), tumor cell proliferation,

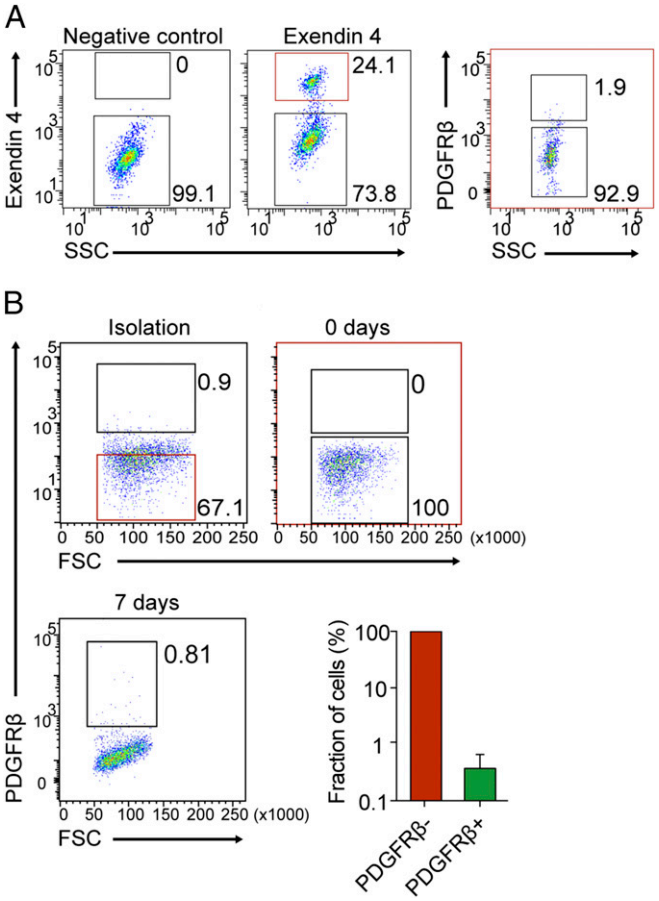

Fig. 8. Rapid conversion of PDGFRβ$^-$ cells to PDGFRβ$^+$ cells occurs in vitro and in vivo. (*A*) Flow cytometry analysis of tumor cells coexpressing GLP1R and PDGFRβ from tumors originated from transplanted PDGFRβ$^-$ βTC3 cells. (*B*) Flow cytometry-gating strategy for sorting PDGFRβ$^-$ tumor cells from parental βTC3 cells. The proportion of PDGFRβ$^+$ βTC3 was analyzed immediately after sorting (0 d, dot plot) and after 7 d of culture (dot plot and column chart). Error bars show the mean ± SD.

and invasion (26, 29, 30). In human cancers, *PDGFD* up-regulation has been documented for prostate, lung, renal, ovarian, brain, breast, and pancreatic cancers (31, 32). However, the mechanisms underlying the effect of PDGF-DD on tumor growth are still largely unknown.

Our study revealed that disruption of PDGF-DD signaling greatly delayed PanNET development in RIP1-TAg2 mice. Genetic loss of a single copy of the gene encoding *Pdgfd* was sufficient to significantly retard tumor growth. The reduction in tumor burden was associated with decreased tumor cell proliferation and prolonged survival of *Pdgfd*-deficient RIP1-TAg2 mice.

As previously reported for PDGF-BB (33, 34), the other known ligand for PDGFRβ, ECs in tumors from RIP1-TAg2 mice appear to be the major source for PDGF-DD. The effect of EC-secreted factors on the regulation of tissue and tumor growth has recently been highlighted (35–37), emphasizing the potential benefit of targeting the cross talk between ECs and tumor cells to supplement conventional antiangiogenic therapies. However, we do not exclude that there may be additional cells in the tumor microenvironment that express low levels of *Pdgfd*. Indeed, *PDGFD* expression has also been documented by malignant cells in ovarian, lung, breast, prostate, renal, and brain tumor-derived cell lines (10, 29, 38, 39).

In tumors, PDGFRβ is expressed mainly by mesenchymal cells, i.e., fibroblasts and pericytes (2, 40). The role of PDGF-BB in the recruitment of pericytes to blood vessels has been well established in tumors from RIP1-TAg2 mice (16). Also, *Pdgfd* overexpression in an orthotopic model of renal cell carcinoma resulted in increased perivascular cell coverage (26). In our model, however, there was no measurable effect on stromal-cell (pericyte) recruitment upon disruption of PDGF-DD signaling. Up-regulation of *Pdgfb* in tumors from RIP1-TAg2;*Pdgfd*$^{-/-}$ mice compared with the wild-type littermates suggests that PDGF-BB exerts a compensatory effect for the loss of PDGF-DD in the present context. The apparent need for compensation by PDGF-BB implies a yet uncharted functional role for PDGF-DD in the tumor stroma. In addition, the sharp decrease in tumor burden caused by *Pdgfd* deficiency strongly supports that compensation by PDGF-BB is only partially attained and that the functions of PDGF-BB and PDGF-DD within the context of tumorigenesis are only partly overlapping. Indeed, stimulation of a PanNET cell line with PDGF-DD, but not with PDGF-BB, increased proliferation and improved sphere-forming capacity. Given the fact that genetic studies have demonstrated closely related phenotypes of mice deficient for *Pdgfb* and *Pdgfrβ* (41, 42), it is tempting to speculate that the unique functions of PDGF-DD are the result of binding to a distinct (co)-receptor that modulates the response of PDGFRβ.

PDGF-DD and PDGF-BB share a conserved growth factor core domain motif, but contrary to PDGF-DD, PDGF-BB carries a basic retention motif domain, allowing binding to heparan sulfate proteoglycans present in the extracellular matrix (15). In contrast, the latent full-length form of PDGF-DD has been suggested to be freely diffusible (43). It is thus reasonable to assume that PDGF-DD has a distinct distribution in the tumor stroma, being able to reach non-vessel-associated PDGFRβ-expressing cells. Therefore, we explored the possibility that nonvascular cell types in the tumor parenchyma of RIP1-TAg2 mice expressed PDGFRβ and constituted potential targets for PDGF-DD. A study of pancreatic islet regeneration demonstrated that immature mouse pancreatic β-cells express PDGFRα and PDGFRβ, signaling by which is required for sustained cell proliferation and islet expansion (44). In agreement, we identified a rare population of malignant cells expressing PDGFRβ in primary tumors and metastatic lesions of RIP1-TAg2 mice. Notably, PDGFRβ$^+$ tumor cells were more abundant in early metastatic lesions in the liver, suggesting that this particular subset of malignant cells may be involved in establishing distant metastases. However, PDGF-DD evidently did not contribute to dissemination as such, because we did not detect any difference in the incidence of hepatic metastatic lesions.

When sorted and transplanted into NOD-SCID mice at quantities down to 200 cells, βTC3 cells were able to recapitulate the morphology and heterogeneity found in tumors from RIP1-TAg2 mice, regardless of the expression of PDGFRβ, evidencing the conserved malignant phenotype of all subsets of cancer cells within this cell line. Although PDGFRβ$^+$ malignant cells held some features of tumor-initiating cells, we could not demonstrate that this was an exclusive or general trait of the subpopulation expressing PDGFRβ. The fact that we were able to identify minor subpopulations of β-cells even in late passages of βTC cell lines led us to consider that the presence of PDGFRβ–expressing βTC3 cells is necessary for the maintenance of the bulk tumor cell population. The coexistence of subpopulations of tumor cells with distinct phenotypic and functional properties within the same tumor points to the existence of uncharted cellular interactions or pathways that contribute to tumor growth and dissemination. Studies in renal cell carcinoma (45) and lung adenocarcinoma (46) have revealed substantial intratumoral heterogeneity as a result of subclonal driver events. Additional studies establish that interactions between genetically distinct subclones of tumor cells are necessary for maintaining tumor heterogeneity (47) and that even minor subpopulations of tumor cells may promote bulk tumor growth

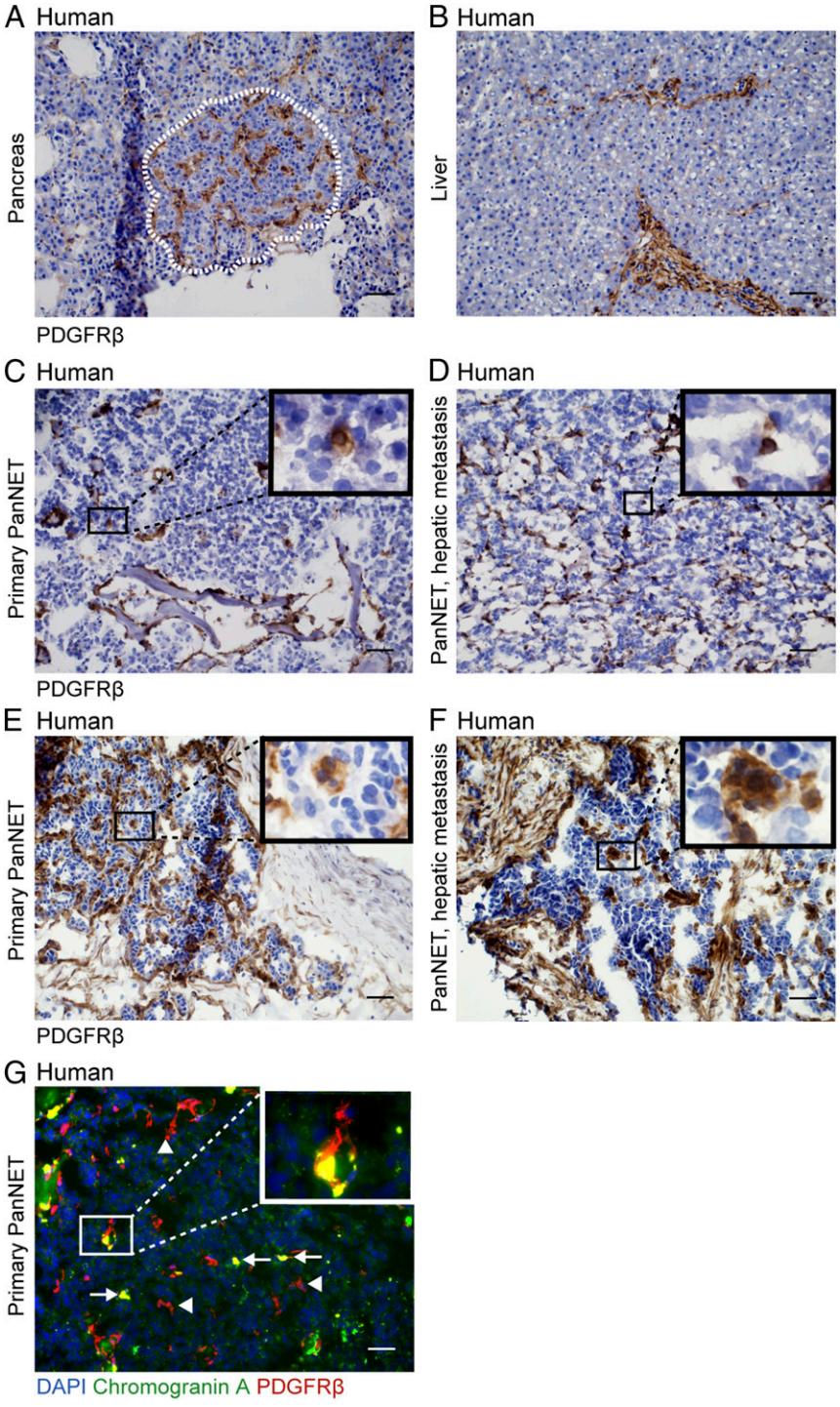

Fig. 9. Human PanNETs harbor a subset of PDGFRβ$^+$ malignant cells. PDGFRβ expression assessed by IHC in (*A*) normal human pancreatic islet and (*B*) liver and in primary and hepatic PanNET expressing (*C* and *D*) low to (*E* and *F*) moderate levels of PDGFRβ in tumor cells. (*G*) Costaining of a primary PanNET with antibodies against PDGFRβ (red) and a neuroendocrine tumor cell marker, Chromogranin A (green). Cell nuclei were stained with DAPI. Representative images are shown. Arrows point out PDGFRβ/chromogranin A double-positive malignant cells; arrowheads point out PDGFRβ single-positive pericytes. (Scale bars, 50 μm.)

via mechanisms of non-cell–autonomous stimulation (48). Thus, one might hypothesize that the cross talk between PDGFRβ$^+$ and PDGFRβ$^-$ malignant clones is necessary for more efficient tumor propagation. Indeed, we found that stimulation of PanNET cells with PDGF-DD in vitro engaged PDGFRβ$^+$ cells in paracrine cross talk with neighboring PDGFRβ$^-$ cells through the induction of mitogenic factors, the identity of which should be corroborated in vivo. A recent study using βTC cells from RIP1-TAg2 mice as a model demonstrates that artificial tumor heterogeneity is the result of stable coexistence of different clones, even without a strict interdependence between subclones (49). We should also consider the prospect that expression of PDGFRβ in malignant cells is due to interconversion between malignant cell populations, e.g., as a result of PDGF-DD-stimulated EMT. In support of this train of

thought, maintenance of a pure PDGFRβ$^-$ cell culture led to rapid reestablishment of the original frequencies of PDGFRβ$^-$ and PDGFRβ$^+$ subclones, in close agreement with studies of subsets of breast cancer cells that hold the ability to spontaneously interconvert (50).

Consistently, we were able to confirm the presence of a rare population of tumor cells expressing PDGFRβ also in human primary and metastatic PanNET. Our findings are supported by previous studies showing that besides stromal cells, human primary PanNET and metastatic cells express high levels of PDGFRβ compared with normal tissue (51, 52). Moreover, clinical reports show evidence of PDGFR activation and copy number alteration in small intestine, gastroenteropancreatic, and pancreatic NET, although the use of whole tumor cell lysates precludes identification of the cell type expressing PDGFRβ (21, 53). The identification of PDGFRβ$^+$ tumor cells in human PanNET has important clinical implications, considering that sunitinib, a PDGFR/VEGFR small molecule inhibitor, was recently approved to treat patients with progressive well-differentiated PanNET (54). Preclinical studies suggest that the therapeutic efficacy of sunitinib is derived from dual targeting of endothelial cells and pericytes (12, 55), but given our finding of the functional importance of PDGF-DD/PDGFRβ for maintaining a functional malignant cell heterogeneity, direct inhibitory effects on tumor cells cannot be excluded.

Altogether, we provide strong evidence for the importance of PDGF-DD for PanNET growth. Moreover, we have identified a subpopulation of PDGFRβ$^+$ malignant β-cells responsive to PDGF-DD in PanNET from an instructive mouse model, and in human primary and hepatic metastatic lesions. Our study thus provides evidence for a functional heterogeneity that needs to be explored to fully understand the tumorigenic process in PanNET.

Materials and Methods

A detailed description of additional procedures can be found in *Supporting Information*.

Animal Care. All experimental procedures involving mice were approved by the Stockholm North and Malmö/Lund committees for animal care (permits N96/11 and M142/13). RIP1-TAg2 transgenic mice were crossed with *Pdgfd*$^{-/-}$ and *Pdgfd*$^{+/-}$ mice or with PDGFRβ-EGFP mice (a kind gift from Christer Betsholtz, Uppsala University, Uppsala, Sweden) on the C57BL/6 background. RIP1-TAg2;*Pdgfd*$^{+/+}$ littermates were used as controls. From 10 wk of age, all RIP1-TAg2 mice received 5% (wt/vol) sugar water to counteract symptoms of hypoglycemia.

Assessment of Angiogenic Islets, Tumor Burden, and Lesion Frequency. Pancreata of 12-wk-old mice were analyzed for the number of angiogenic islets, counted under a stereological microscope, and defined as islets with red patches and $<1 \times 1$ mm. Tumors were defined as $>1 \times 1$ mm and were excised, counted, and measured with a caliper to obtain the total number of tumors and total tumor volume in each RIP1-TAg2 mouse. Tumor volume was calculated as length $\times$ width$^2 \times \pi/6$.

Mouse Tissue Preparation. Mice were anesthetized, the heart perfused with PBS followed by 4% (wt/vol) paraformaldehyde (PFA). For paraffin embedding, pancreata and livers were kept in PFA at 4 °C overnight followed by paraffin embedding. For cryopreservation, organs were kept in 30% sucrose at 4 °C overnight followed by embedding in optimal cutting temperature (OCT) cryomount (Histolab).

Quantification of Tumor Cell Proliferation. Mice were injected intraperitoneally with 100 μg/g body weight of 5-Bromo-2′-deoxyuridine (BrdU; Sigma-Aldrich) and kept for 2 h before being euthanized. Pancreata were sectioned and stained with primary antibody against BrdU (1:100; Accurate Chemical). Cells with incorporated BrdU were quantified as the fraction of positively stained cells per total number of cells.

Fluorescence-Activated Cell Sorting and Analysis. For procedures of preparation of cells for flow cytometry, please refer to *Supporting Information*. Cells were sorted using a BD FACSARIAIII sorter with BD FACSDiva software or analyzed on BD FACSCantoII or BD FACSVerse flow cytometers (all from Beckton Dickinson Immunocytometry Systems). Further analysis of acquired cells was performed using FlowJo software (FlowJo LLC).

RNA Isolation and Gene Expression Profiling. Total RNA from cultured cells and tumor lysates was isolated using the RNeasy mini kit (QIAGEN) according to the manufacturer's instructions followed by cDNA synthesis using the iScript cDNA synthesis kit (Bio-Rad Laboratories). Quantitative RT-PCR was performed as described before (56). Expression levels were calculated relative to the ribosomal housekeeping gene RPL19 as $100 \times 2^{-\Delta Ct}$. For primers, refer to *Supporting Information*.

Statistical Analysis. Data are shown as mean ± SD. Statistical analysis comparing means was performed using the unpaired, two-tailed Student's *t* test; analysis of proportions was performed using the χ^2 test; analysis of survival was performed using the log rank test; and in all cases, statistical significance was defined as $P < 0.05$.

ACKNOWLEDGMENTS. K.P. is the Göran and Birgitta Grosskopf Professor at Lund University. The research presented herein is supported by a Consolidator Grant from the European Research Council (the TUMORGAN project), the Swedish Research Council, the Swedish Cancer Society, the STARGET consortium (a Swedish Research Council Linnaeus network), BioCARE, and Lund University.

1. Hanahan D, Weinberg RA (2011) Hallmarks of cancer: The next generation. *Cell* 144(5):646–674.
2. Cortez E, Roswall P, Pietras K (2014) Functional subsets of mesenchymal cell types in the tumor microenvironment. *Semin Cancer Biol* 25:3–9.
3. Gerlinger M, et al. (2012) Intratumor heterogeneity and branched evolution revealed by multiregion sequencing. *N Engl J Med* 366(10):883–892.
4. Heldin C-H, Westermark B (1999) Mechanism of action and in vivo role of platelet-derived growth factor. *Physiol Rev* 79(4):1283–1316.
5. Pietras K, Sjöblom T, Rubin K, Heldin CH, Ostman A (2003) PDGF receptors as cancer drug targets. *Cancer Cell* 3(5):439–443.
6. Demetri GD, et al. (2002) Efficacy and safety of imatinib mesylate in advanced gastrointestinal stromal tumors. *N Engl J Med* 347(7):472–480.
7. Druker BJ, et al. (2001) Activity of a specific inhibitor of the BCR-ABL tyrosine kinase in the blast crisis of chronic myeloid leukemia and acute lymphoblastic leukemia with the Philadelphia chromosome. *N Engl J Med* 344(14):1038–1042.
8. Andrae J, Gallini R, Betsholtz C (2008) Role of platelet-derived growth factors in physiology and medicine. *Genes Dev* 22(10):1276–1312.
9. Bergsten E, et al. (2001) PDGF-D is a specific, protease-activated ligand for the PDGF beta-receptor. *Nat Cell Biol* 3(5):512–516.
10. LaRochelle WJ, et al. (2001) PDGF-D, a new protease-activated growth factor. *Nat Cell Biol* 3(5):517–521.
11. Hanahan D (1985) Heritable formation of pancreatic β-cell tumours in transgenic mice expressing recombinant insulin/simian virus 40 oncogenes. *Nature* 315(6015):115–122.
12. Bergers G, Song S, Meyer-Morse N, Bergsland E, Hanahan D (2003) Benefits of targeting both pericytes and endothelial cells in the tumor vasculature with kinase inhibitors. *J Clin Invest* 111(9):1287–1295.
13. Anderberg C, et al. (2013) Deficiency for endoglin in tumor vasculature weakens the endothelial barrier to metastatic dissemination. *J Exp Med* 210(3):563–579.
14. Wu Q, et al. (2013) Emerging roles of PDGF-D in EMT progression during tumorigenesis. *Cancer Treat Rev* 39(6):640–646.
15. Lindblom P, et al. (2003) Endothelial PDGF-B retention is required for proper investment of pericytes in the microvessel wall. *Genes Dev* 17(15):1835–1840.
16. Xian X, et al. (2006) Pericytes limit tumor cell metastasis. *J Clin Invest* 116(3):642–651.
17. Song S, Ewald AJ, Stallcup W, Werb Z, Bergers G (2005) PDGFRbeta+ perivascular progenitor cells in tumours regulate pericyte differentiation and vascular survival. *Nat Cell Biol* 7(9):870–879.
18. Franco M, Pàez-Ribes M, Cortez E, Casanovas O, Pietras K (2011) Use of a mouse model of pancreatic neuroendocrine tumors to find pericyte biomarkers of resistance to anti-angiogenic therapy. *Horm Metab Res* 43(12):884–889.
19. Uutela M, et al. (2004) PDGF-D induces macrophage recruitment, increased interstitial pressure, and blood vessel maturation during angiogenesis. *Blood* 104(10):3198–3204.
20. Nozawa H, Chiu C, Hanahan D (2006) Infiltrating neutrophils mediate the initial angiogenic switch in a mouse model of multistage carcinogenesis. *Proc Natl Acad Sci USA* 103(33):12493–12498.
21. Duerr EM, et al. (2008) Defining molecular classifications and targets in gastroenteropancreatic neuroendocrine tumors through DNA microarray analysis. *Endocr Relat Cancer* 15(1):243–256.
22. Tornehave D, Kristensen P, Rømer J, Knudsen LB, Heller RS (2008) Expression of the GLP-1 receptor in mouse, rat, and human pancreas. *J Histochem Cytochem* 56(9):841–851.
23. Gong S, et al. (2003) A gene expression atlas of the central nervous system based on bacterial artificial chromosomes. *Nature* 425(6961):917–925.
24. Efrat S, et al. (1988) Beta-cell lines derived from transgenic mice expressing a hybrid insulin gene-oncogene. *Proc Natl Acad Sci USA* 85(23):9037–9041.

25. O'Connor DT, Deftos LJ (1986) Secretion of chromogranin A by peptide-producing endocrine neoplasms. *N Engl J Med* 314(18):1145–1151.
26. Xu L, Tong R, Cochran DM, Jain RK (2005) Blocking platelet-derived growth factor-D/platelet-derived growth factor receptor beta signaling inhibits human renal cell carcinoma progression in an orthotopic mouse model. *Cancer Res* 65(13):5711–5719.
27. Kong D, et al. (2009) miR-200 regulates PDGF-D-mediated epithelial-mesenchymal transition, adhesion, and invasion of prostate cancer cells. *Stem Cells* 27(8):1712–1721.
28. Kong D, et al. (2008) Platelet-derived growth factor-D overexpression contributes to epithelial-mesenchymal transition of PC3 prostate cancer cells. *Stem Cells* 26(6):1425–1435.
29. Liu J, et al. (2011) PDGF-D improves drug delivery and efficacy via vascular normalization, but promotes lymphatic metastasis by activating CXCR4 in breast cancer. *Clin Cancer Res* 17(11):3638–3648.
30. Li H, Fredriksson L, Li X, Eriksson U (2003) PDGF-D is a potent transforming and angiogenic growth factor. *Oncogene* 22(10):1501–1510.
31. Ustach CV, et al. (2004) A potential oncogenic activity of platelet-derived growth factor d in prostate cancer progression. *Cancer Res* 64(5):1722–1729.
32. Wang Z, et al. (2010) Emerging roles of PDGF-D signaling pathway in tumor development and progression. *Biochim Biophys Acta* 1806(1):122–130.
33. Abramsson A, Lindblom P, Betsholtz C (2003) Endothelial and nonendothelial sources of PDGF-B regulate pericyte recruitment and influence vascular pattern formation in tumors. *J Clin Invest* 112(8):1142–1151.
34. Franco M, Roswall P, Cortez E, Hanahan D, Pietras K (2011) Pericytes promote endothelial cell survival through induction of autocrine VEGF-A signaling and Bcl-w expression. *Blood* 118(10):2906–2917.
35. Butler JM, Kobayashi H, Rafii S (2010) Instructive role of the vascular niche in promoting tumour growth and tissue repair by angiocrine factors. *Nat Rev Cancer* 10(2):138–146.
36. Cao Z, et al. (2014) Angiocrine factors deployed by tumor vascular niche induce B cell lymphoma invasiveness and chemoresistance. *Cancer Cell* 25(3):350–365.
37. Seton-Rogers S (2014) Microenvironment: Endothelial cells create a niche. *Nat Rev Cancer* 14(5):298.
38. Uutela M, et al. (2001) Chromosomal location, exon structure, and vascular expression patterns of the human PDGFC and PDGFD genes. *Circulation* 103(18):2242–2247.
39. Lokker NA, Sullivan CM, Hollenbach SJ, Israel MA, Giese NA (2002) Platelet-derived growth factor (PDGF) autocrine signaling regulates survival and mitogenic pathways in glioblastoma cells: Evidence that the novel PDGF-C and PDGF-D ligands may play a role in the development of brain tumors. *Cancer Res* 62(13):3729–3735.
40. Pietras K, Ostman A (2010) Hallmarks of cancer: Interactions with the tumor stroma. *Exp Cell Res* 316(8):1324–1331.
41. Levéen P, et al. (1994) Mice deficient for PDGF B show renal, cardiovascular, and hematological abnormalities. *Genes Dev* 8(16):1875–1887.
42. Soriano P (1994) Abnormal kidney development and hematological disorders in PDGF beta-receptor mutant mice. *Genes Dev* 8(16):1888–1896.
43. Ehnman M, Li H, Fredriksson L, Pietras K, Eriksson U (2009) The uPA/uPAR system regulates the bioavailability of PDGF-DD: Implications for tumour growth. *Oncogene* 28(4):534–544.
44. Chen H, et al. (2011) PDGF signalling controls age-dependent proliferation in pancreatic β-cells. *Nature* 478(7369):349–355.
45. Gerlinger M, et al. (2014) Genomic architecture and evolution of clear cell renal cell carcinomas defined by multiregion sequencing. *Nat Genet* 46(3):225–233.
46. Zhang J, et al. (2014) Intratumor heterogeneity in localized lung adenocarcinomas delineated by multiregion sequencing. *Science* 346(6206):256–259.
47. Inda MM, et al. (2010) Tumor heterogeneity is an active process maintained by a mutant EGFR-induced cytokine circuit in glioblastoma. *Genes Dev* 24(16):1731–1745.
48. Marusyk A, et al. (2014) Non-cell-autonomous driving of tumour growth supports sub-clonal heterogeneity. *Nature* 514(7520):54–58.
49. Archetti M, Ferraro DA, Christofori G (2015) Heterogeneity for IGF-II production maintained by public goods dynamics in neuroendocrine pancreatic cancer. *Proc Natl Acad Sci USA* 112(6):1833–1838.
50. Gupta PB, et al. (2011) Stochastic state transitions give rise to phenotypic equilibrium in populations of cancer cells. *Cell* 146(4):633–644.
51. Fjällskog ML, Lejonklou MH, Oberg KE, Eriksson BK, Janson ET (2003) Expression of molecular targets for tyrosine kinase receptor antagonists in malignant endocrine pancreatic tumors. *Clin Cancer Res* 9(4):1469–1473.
52. Fjällskog ML, Hessman O, Eriksson B, Janson ET (2007) Upregulated expression of PDGF receptor beta in endocrine pancreatic tumors and metastases compared to normal endocrine pancreas. *Acta Oncol* 46(6):741–746.
53. Banck MS, et al. (2013) The genomic landscape of small intestine neuroendocrine tumors. *J Clin Invest* 123(6):2502–2508.
54. Raymond E, et al. (2011) Sunitinib malate for the treatment of pancreatic neuroendocrine tumors. *N Engl J Med* 364(6):501–513.
55. Pietras K, Hanahan D (2005) A multitargeted, metronomic, and maximum-tolerated dose "chemo-switch" regimen is antiangiogenic, producing objective responses and survival benefit in a mouse model of cancer. *J Clin Oncol* 23(5):939–952.
56. Cunha SI, et al. (2010) Genetic and pharmacological targeting of activin receptor-like kinase 1 impairs tumor growth and angiogenesis. *J Exp Med* 207(1):85–100.